Available online at www.sciencedirect.com
ScienceDirect
Journal of Catalysis 245 (2007) 45–54
JOURNAL OF CATALYSIS
www.elsevier.com/locate/jcat

Study of $Ir/WO_3/ZrO_2–SiO_2$ ring opening catalysts Part I: Characterization

Sebastien Lecarpentier, Jacob van Gestel, Karine Thomas, Marwan Houalla *

Laboratoire Catalyse et Spectrochimie (UMR CNRS 6506), ENSICAEN-Université de Caen, 6 Bd. Maréchal Juin, 14050 Caen (cedex), France

Received 7 July 2006; revised 6 September 2006; accepted 8 September 2006

Available online 24 October 2006

Abstract

This paper is the first part of a systematic study of the influence of W and Ir loading on the activity of $Ir/WO_3/ZrO_2–SiO_2$ catalysts for the ring-opening reaction of naphthenic molecules using methylcyclohexane (MCH) as a model compound. A series of Si-stabilized tungstated zirconias, $WO_x/ZrO_2–SiO_2$, containing up to 3.5 at W/nm^2 was prepared. Ir-based catalysts containing up to 1.2 wt% were obtained by impregnation of these solids. The acidity of Si-stabilized tungstated zirconias, ZSiWx, was monitored by low-temperature CO adsorption followed by infrared (IR) spectroscopy. The results indicated the development of strong and relatively strong Brønsted acidity with increasing W surface density above a threshold of 1 atom W/nm^2. The study of the Ir-doped solids showed that the texture, structure, and acidity of the ZSiWx solids were not affected by Ir deposition. The characterization of the metallic function was performed by hydrogenation of toluene and by CO adsorption at ambient temperature, followed by IR spectroscopy. Both methods indicated a low and constant Ir dispersion for the yIr/ZSiW0 ($y = 0.3$, 0.6, 1.2) series. For a given Ir loading (1.2Ir/ZSiWx), a progressive decrease in the dispersion of Ir metal with increasing W surface density was observed.

Keywords: Tungstated zirconia; Iridium; Toluene hydrogenation; Infrared measurements; CO adsorption

1. Introduction

The conversion of light cycle oil feedstock to diesel fuel products requires deep desulfurization and hydrogenation, followed by ring opening of the naphthenic cycles to form alkanes (molecules with higher cetane indices). In general, opening of a C_6 six-membered naphthenic ring is more difficult than opening of a C_5 ring [1–3]. Thus, a suitable catalyst must contain an acid function to allow for ring contraction. The cleavage of a C–C bond is then performed by hydrogenolysis over the metal. To date, no systematic study of the influence of acidity and metal content on C_6 ring-opening activity has been performed. Previous studies have shown that the acidity of zirconia can be modulated with deposition of a controlled amount of W [4]. Thus, a catalytic system consisting of tungstated zirconias and a metal with strong C–C bond cleavage activity, such as Ir, appears promising. This paper is the first part of a systematic study of the influence of W and Ir loading on the catalyst activity for ring-opening of naphthenic molecules using methylcyclohexane (MCH) as a model compound.

The objectives of the present study are to characterize the evolution of the acidity of tungstated zirconia with W surface density and to analyze the dispersion of the Ir phase as a function of W deposition. Evolution of the acidity was monitored by low-temperature CO adsorption followed by infrared (IR) spectroscopy. Dispersion of the Ir phase was examined by IR study of CO adsorption at ambient temperature and catalytic hydrogenation of toluene.

2. Experimental

2.1. Materials

Zirconia doped with 1.2 wt% silica was prepared by dropwise addition of a 10 M aqueous solution of ammonia to a 0.2 M solution of zirconyl chloride octahydrate ($ZrOCl_2$, Fluka) up to a pH of 9.9. Preliminary experiments indicated that sub-

* Corresponding author. Fax: +33 2 31 45 28 22.
E-mail address: marwan.houalla@ensicaen.fr (M. Houalla).

0021-9517/$ – see front matter
doi:10.1016/j.jcat.2006.09.018

stantial stabilisation of the surface of the zirconia support can be achieved with the incorporation of 1.2 wt% Si. Thus subsequent studies of the influence of calcination temperature and W deposition were conducted with this solid. The silicon was introduced before precipitation using the prerequisite amount of liquid $SiCl_4$, (99.8%, Acros Organics). The precipitated material was heated at 363 K for 48 h and then maintained at room temperature for 96 h in the solution. The final product was recovered by vacuum filtration. It was then redispersed in deionised water to remove residual chlorine and filtered. This operation was repeated until no traces of Cl^- could be detected with an $AgNO_3$ solution. The washed product was dried at 393 K for 16 h and calcined in air at 1023 K for 3 h. Completion of the experiments included in the present work required the synthesis of two batches of ZrO_2. The differences in the characteristics of the supports thus obtained were minor and did not significantly affect the results.

The W phase (0–12 wt% W) was deposited by impregnation of the support using ammonium metatungstate solution, followed by calcination at 1023 K for 3 h. The Ir (0–1.2 wt%) was added by incipient wetness impregnation with a basic iridium chloride solution (pH 9), followed by calcination at 723 K with a 20% O_2 + 80% N_2 flow of 25 ml/min. The catalyst was reduced in situ in flowing H_2 at 623 K at atmospheric pressure before use. Tungstated zirconias were designated as ZSiWx, where x is the W surface density expressed as at W/nm^2. The series of Ir deposited on tungstated zirconia was denoted as yIr/ZSiWx, where y is the nominal percentage of Ir in the catalysts.

2.2. BET surface area and pore volume

The specific surface area of the catalyst was determined from physical adsorption of N_2 at 77 K by applying the BET equation on the part of the adsorption isotherm with $0.05 \leqslant p/p_0 \leqslant 0.35$. The adsorption isotherms were measured in a Micromeritics ASAP 2000 apparatus. The samples were first outgassed at 573 K in dynamic vacuum for 1 h. The total pore volume was determined at $p/p_0 = 0.99$.

2.3. X-ray diffraction

Powder X-ray diffraction spectra were recorded with a Philips PW1750 spectrometer using Cu$K\alpha$ radiation. The angle (2θ) was varied from 20° to 70° with steps of 0.02° measured for 10 s. The zirconia phase can be characterized by the specific reflections ($11\bar{1}$) at $2\theta = 28.2°$ and (111) at $2\theta = 31.5°$ for the monoclinic phase and (111) at $2\theta = 30.2°$ for the tetragonal phase. The fraction of the monoclinic phase was estimated using the formula proposed by Toraya et al. [5], and the crystallite size was calculated from the (111) line at $2\theta \sim 30°$ using the Debye–Scherrer formula [6]. The crystalline structure of the present phases was identified through comparison with the database of the Joint Committee on Powder Diffraction Standards (JCPDS).

2.4. IR experiments

The IR spectra were recorded on a Nicolet Nexus FTIR spectrophotometer equipped with a DTGS detector. The powder was pressed into a self-supported wafer (~20 mg). Activation of the wafer was carried out in situ in an IR cell under flowing dry air at 673 K for 2 h. Then the pellet was treated under dry hydrogen at 623 K for 1 h, cooled to 473 K, evacuated for 2 h, and cooled to room temperature. All spectra were normalized to 20 mg of the solid. Adsorption of CO probe molecule was performed at room temperature to determine the dispersion of supported metal [7,8] and at 100 K to evaluate the acid strengths of catalysts [9,10].

2.5. Toluene hydrogenation

Hydrogenation of toluene (0.026 bar of toluene) was carried out at 323 K in a dynamic Pyrex reactor under atmospheric pressure. The flow of toluene–hydrogen mixture was 90 cm^3/min. Reaction products were analysed using a 50-m Chrompack CP-Sil 5CB column and a flame ionization detector. The mass was adjusted to obtain a conversion <7%, in order to calculate the initial rate. Before catalytic testing, the catalyst was activated in flowing air at 673 K for 2 h and reduced at 623 K in flowing hydrogen for 1 h.

3. Results

3.1. Texture and composition of the ZSiWx solids

Table 1 summarizes the characteristics of various tungstated zirconia catalysts. The specific surface area of the solids was ca. 115 ± 15 m^2/g. The W surface density was calculated assuming that the measured surface area is due to the support.

3.2. Crystalline composition of the support

Fig. 1 shows the XRD patterns for the support (ZSiW0) and tungstated zirconia solids (ZSiWx). The spectra of the ZSiWx solids (x = 0.4, 0.9, 2.5) show only the lines characteristic of the tetragonal form of zirconia ($2\theta = 30.2°$, 35.4°, 50.6°, 60.4°); those of the remaining solids (x = 0, 1.5, 3.4) also show an additional line at $2\theta = 28.2°$, characteristic of the monoclinic form (($11\bar{1}$) plane). The percentage of the monoclinic phase present was estimated at 9% [5].

Table 1
Composition and texture of various ZSiWx catalysts

Solid	W loading (wt% W)	Surface area (m^2/g_{cat})	V_p (cm^3/g_{cat})	Surface (m^2/g_{ZrO_2})	Density (at W/nm^2)
ZSiW0	0	97	0.29	97	0
ZSiW0.4	1.5	129	0.25	132	0.4
ZSiW0.9	3.7	125	0.25	132	0.9
ZSiW1.5	4.3	91	0.28	96	1.5
ZSiW1.9	7.6	120	0.25	133	1.9
ZSiW2.5	8.4	99	0.23	111	2.5
ZSiW3.4	11.8	98	0.24	115	3.4

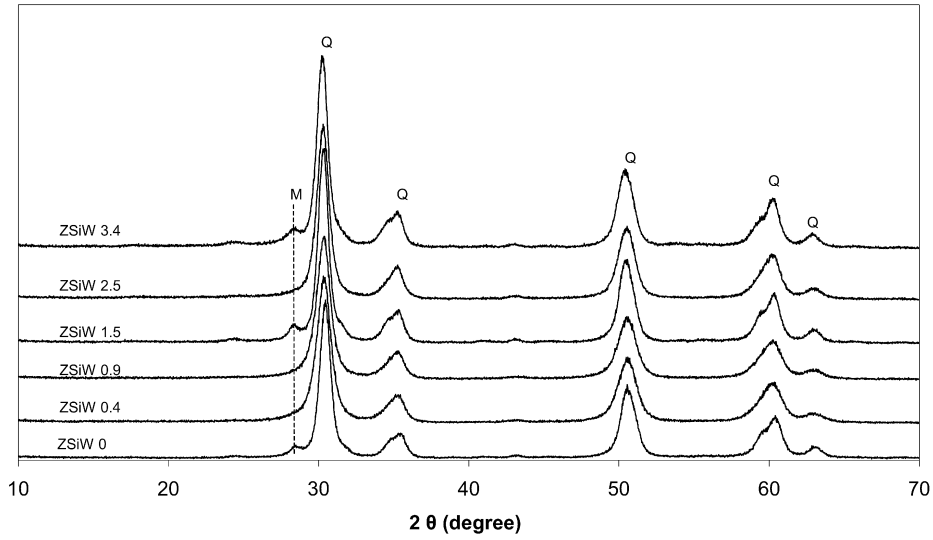

Fig. 1. XRD patterns for Si-stabilized zirconia (ZSiW0) and tungstated zirconia (ZSiWx) catalysts.

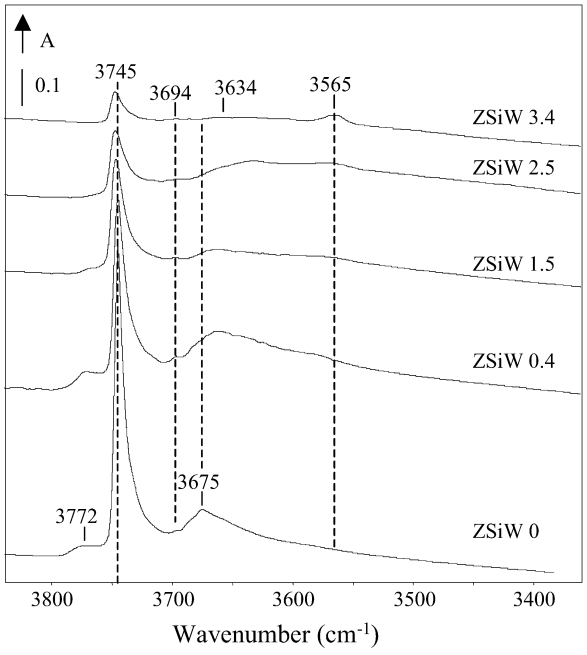

Fig. 2. FTIR spectra of ZSiWx solids in the hydroxyl region.

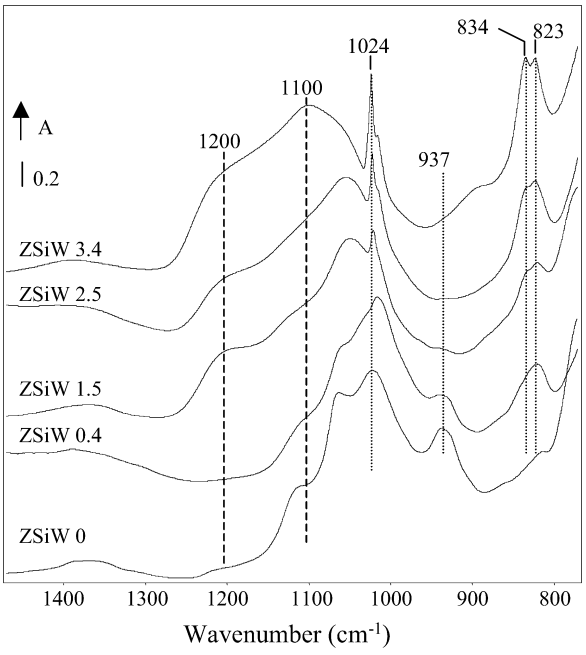

Fig. 3. FTIR spectra of ZSiWx solids in the 770–1470 cm^{-1} region.

3.3. Characterization of the ZSiWx solids by FTIR

Fig. 2 shows the IR spectra for the support and ZSiWx solids in the hydroxyl region. The IR spectrum of the modified zirconia support ZSiW0 exhibited bands at 3772, 3745, 3694, and 3675 cm^{-1}. The most intense band located at 3745 cm^{-1} is attributed to isolated silanols, Si–OH. The bands at 3772 and 3675 cm^{-1} were assigned respectively to the O–H stretching vibrations of isolated type I (Zr^{4+}–OH) and bridged type II [$(Zr^{4+})_2$OH or $(Zr^{4+})_3$OH] hydroxyls [11,12]. The band at 3694 cm^{-1} has not yet been attributed, but appears to be associated with the presence of Si. Increasing the W surface density brings about a decrease in the intensity of the bands characteristics of the hydroxyl groups and a concomitant development of a band at 3565 cm^{-1}. This band is related to the presence of W and can be tentatively ascribed to $(W^{x+})_n$OH perturbed by the support or a bridged W–OH–Zr species.

Fig. 3 shows the IR spectra for the ZSiWx solids in the 1490–760 cm^{-1} region. Note the development of bands (or shoulders) at 1200, 1100, 1024, 1015, 834 and 823 cm^{-1} with increasing W surface density. This is accompanied by a decrease in the intensity of the band located at 937 cm^{-1} attributed to ν(Si–O(H)) vibration. The development of the bands at 834, 823, 1100 and 1200 cm^{-1} appears to reflect the evolution of Si environment form isolated Si to Si in a silica-like environment [13]. The bands at 1024 and 1015 cm^{-1} are attributed to ν(W=O) vibration [4,14].

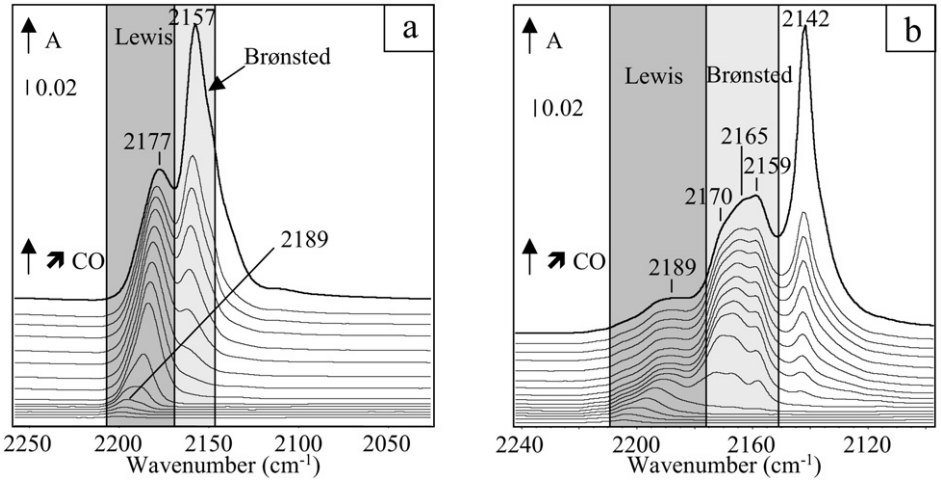

Fig. 4. Infrared spectra for support ZSiW0 (a) and ZSiW3.4 (b) obtained with incremental addition of CO up to 100 Pa at equilibrium.

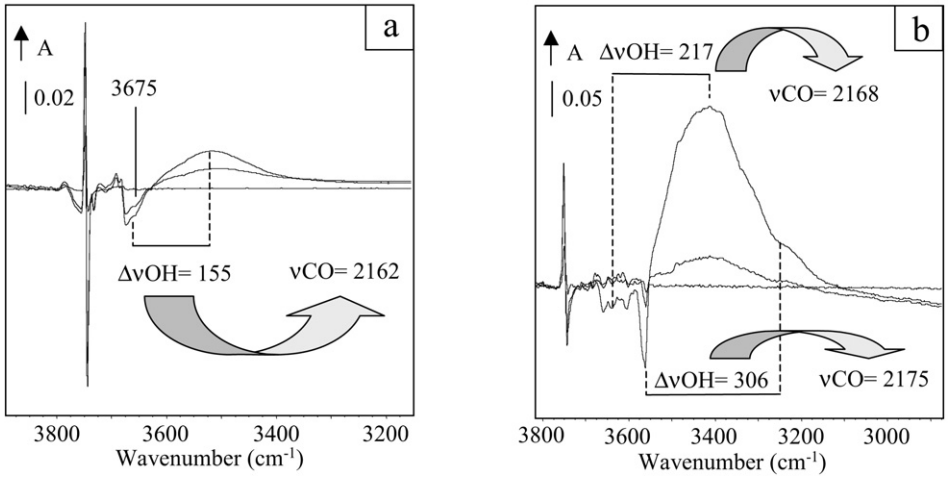

Fig. 5. Infrared spectra of support obtained for the first CO doses that perturb the hydroxyl region for ZSiW0 (a) and ZSiW3.4 (b).

Several probe molecules, including carbon monoxide, pyridine, and lutidine, can be used to characterize the acidity of oxide surfaces. For the present study, carbon monoxide, adsorbed at low temperature, has the advantage of being sensitive to the strength of Brønsted acid sites thus titrated [9,10]. The interaction between CO and the hydroxyl groups leads to a shift to lower wavenumbers of the vibration ν(OH). The magnitude of the shift $\Delta\nu$(OH) is proportional to the strength of the acid site [15]. Thus, analysis of the hydroxyl region between 3000 and 4000 cm^{-1} should allow monitoring of catalyst acidity. The region between 2100 and 2250 cm^{-1} is also of interest for characterizing the acidity, because it includes the stretching vibration of CO molecules interacting with hydroxyl groups or coordinatively unsaturated sites (Lewis acid sites) [16]. The ν(CO) vibration in this region is characteristic of the strength of the acid site probed. A correlation between the position of the ν(CO) vibration and the $\Delta\nu$(OH) shift has been reported [9,17,18].

The distribution of the acid sites was determined from the IR spectra of the catalysts in the presence of 100 Pa of CO at equilibrium. Figs. 4a and 4b show the IR spectra obtained for the solids ZSiW0 and ZSiW3.4 during progressive addition of CO.

The IR spectrum for the Si-stabilized zirconia ZSiW0, exposed to 100 Pa of CO at equilibrium at low temperature (Fig. 4a, top spectrum) shows essentially two bands at 2177 and 2157 cm^{-1} attributed, respectively, to the vibration of CO molecules interacting with Lewis acid sites and weak Brønsted acid sites (silanol groups or hydroxyls) [4,19]. Analysis of the spectra obtained on addition of small doses of CO (Fig. 4a) reveals the presence of a weaker band at around 2189 cm^{-1} attributed to the interaction of CO with relatively stronger Lewis acid sites. The analysis of IR spectra obtained for the first doses of CO (Fig. 5) gives more information with respect to Brønsted acid sites. As indicated earlier, studying the perturbation of the OH region allows assignment of the ν(CO) vibration. Fig. 5a shows a $\Delta\nu$(OH) shift of 155 cm^{-1}. This indicates stronger Brønsted acidity than that reported for alumina [$\Delta\nu$(OH) = 95 cm^{-1}] [20]. According to the correlation, reported by Cairon et al. [9], between the stretching vibration ν(CO) and $\Delta\nu$(OH) of the hydroxyls perturbed by the interaction with CO molecule, such a shift corresponds to a ν(CO) of 2162 cm^{-1}. Thus, the

Table 2
Interaction of CO with hydroxyl groups at 100 K: Shifts $\Delta\nu$OH and νCO

Solid	ν(OH)	$\Delta\nu$(OH)	ν(CO) small dose	ν(CO) 100 Pa	Assignment
ZSiW0	3675	155	2162	2157	$(Zr^{4+})_n$OH (type II)
	3745	100		2157	Si–OH
	3772				Zr^{4+}–OH (type I)
ZSiW3.4	3565	306	2172	2170	See text
	3634	217	2167	2165	See text
	3745			2159	Si–OH

observed ν(CO) vibration at 2162 cm^{-1} (Fig. 4a, Table 2) is associated with ν(OH) vibration at 3675 cm^{-1} related to bridged type II hydroxyls.

The IR spectrum (Fig. 4b) for the Si-stabilized zirconia ZSiW3.4 exposed to 100 Pa of CO at equilibrium is more complex than that for ZSiW0 solid. The development of the band at 2189 cm^{-1} related to Lewis acid shows that the strength of the Lewis acid sites increases with increasing W. However, the area of the band remains significantly lower than that observed at 2177 cm^{-1} for ZSiW0, indicating a decreased abundance of these sites. Analysis of the results obtained from the addition of small doses of CO also points to the presence of a band at higher wavenumber (ca. 2200 cm^{-1}), indicating a minor formation of stronger Lewis acid sites.

IR results also show the development of stronger Brønsted acid sites on addition of W. Thus the IR spectrum (Fig. 4b) for the solid ZSiW3.4 exposed to 100 Pa of CO at equilibrium at low temperature shows bands at ca. 2170, 2165, and 2159 cm^{-1}, compared with 2177 and 2157 cm^{-1} for zirconia. Although the band at around 2170 cm^{-1} is generally ascribed to CO adsorbed on Lewis acid sites, the analysis of OH and CO regions after the addition of first doses of CO (Fig. 5b), suggests that it is more likely due to an interaction of CO with Brønsted acid sites. Indeed, the study of $\Delta\nu$(OH) and ν(CO) vibrations shows that the band at 2172 cm^{-1} (2170 cm^{-1} at saturation) for the catalyst ZSiW3.4 is related to a $\Delta\nu$(OH) shift of 306 cm^{-1}. This shift is attributed to CO in interaction with a hydroxyl group at 3565 cm^{-1}. Based on results reported previously [9], a $\Delta\nu$(OH) shift of 306 cm^{-1} is comparable to that observed for H-ZSM5. Thus, it is indicative of CO interaction with strong Brønsted acid sites. In accordance with the literature [21], the band at ca. 2167 cm^{-1} is attributed to the vibration of CO interacting with relatively strong Brønsted acid sites located at around 3634 cm^{-1} [$\Delta\nu$(OH) shift = 217 cm^{-1}]. For comparison, $\Delta\nu$(OH) shifts of 185 and 265 cm^{-1} were reported for HNaYS and HY zeolites, respectively [9]. The third band at 2158 cm^{-1} is assigned to the interaction of CO with the hydroxyls of the zirconia support and silanols perturbed by adjacent W. With increasing CO doses (Fig. 4b), the ν(CO) vibrations initially at 2172 and 2167 cm^{-1} shifted to lower wavenumbers (2170 and 2165 cm^{-1}). Thus, for the ZSiW3.4 solid, the presence of relatively strong (2167 cm^{-1}) and strong Brønsted acid sites (2172 cm^{-1}) was detected. The results are summarized in Table 2.

Curve fitting of the IR spectral envelope in the 2190–2210 cm^{-1} region was carried out for a more quantitative analysis of the evolution with tungsten density of the intensity of different bands attributed to Brønsted acid sites. Fig. 6 shows an example of the decomposition of the envelope for the solid ZSiW1.5 obtained in the presence of 100 Pa of CO at equilibrium. The envelope, located between 2178 and 2225 cm^{-1} and characteristic of Lewis acid sites, was decomposed into 3 bands at 2199, 2193, and 2186 cm^{-1}. The region between 2140 and 2180 cm^{-1}, indicative of the presence of Brønsted acid sites, was decomposed into 4 bands at 2175, 2167, 2160, and 2148 cm^{-1}. The bands at 2141 and 2135 cm^{-1} were attributed to physisorbed CO. The number of bands and their positions were determined using second derivative results and those of the addition of small increments of CO. A Gaussian profile was used for the bands. The IR spectra for the catalysts in the presence of 100 Pa of CO at equilibrium were decomposed using EXCEL software by minimizing the difference between the experimental and reconstituted spectra. The position of the bands was allowed to vary by ±2 cm^{-1}. The same methodology was used for the decomposition of the IR spectra after CO adsorption for the remaining ZSiWx solids.

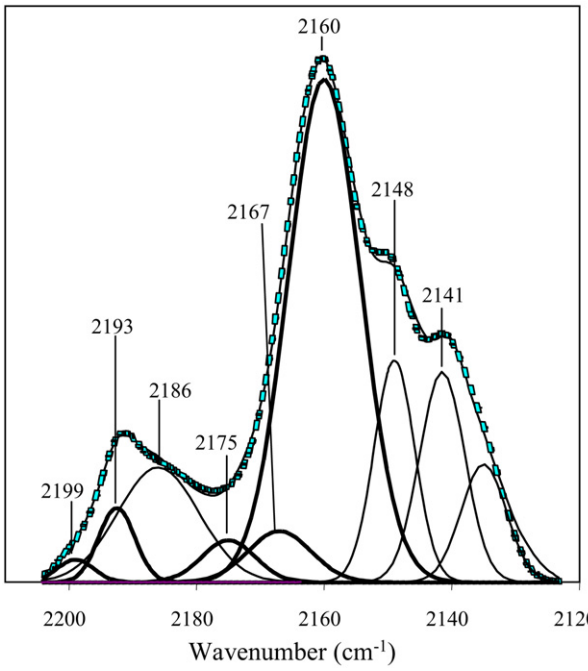

Fig. 6. Example of the decomposition into different Gaussian peaks of the infrared spectrum for the solid ZSiW1.5, in the CO stretching vibration region, following exposure to 100 Pa of CO at equilibrium at low temperature. Continuous line: experimental spectrum; dashed line: reconstituted spectrum.

Fig. 7 shows the areas of the bands characteristic of CO adsorbed on Brønsted acid sites as a function of W surface density. The results indicate that for W surface densities above a threshold value around 1 atom of W/nm^2, the areas of the bands at 2167 and 2175 cm^{-1} increase linearly with increasing W surface density. Thus, a minimum W surface density appears to be required for the development of strong Brønsted acid sites. Note the parallel evolution of the bands at 2175 and 3565 cm^{-1}, which is consistent with the attribution of these bands to the vibrations of CO molecules and hydroxyls in interaction.

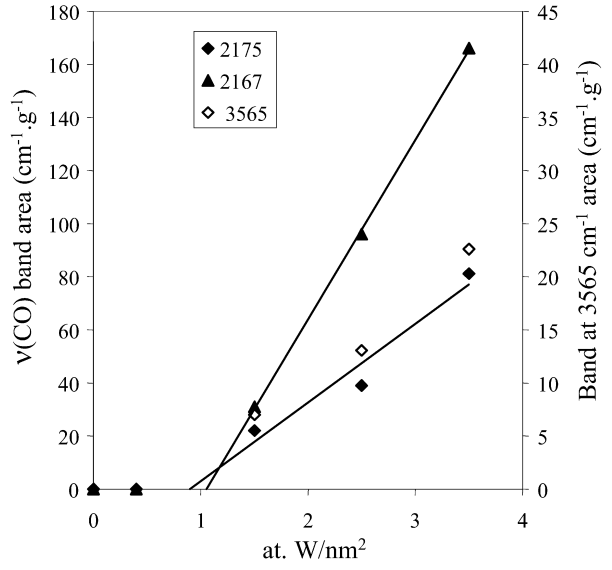

Fig. 7. Evolution of the areas of the infrared bands attributed to CO adsorbed on Brønsted acid sites as a function of W surface density. (◆, ▲) Left scale; (◇) right scale.

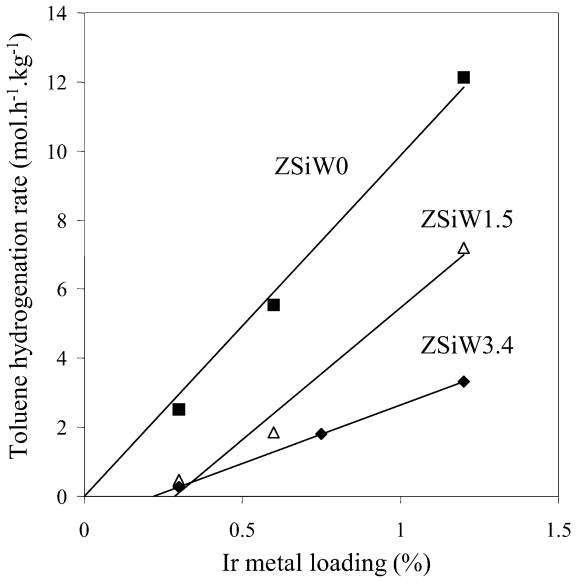

Fig. 8. Evolution of toluene hydrogenation rate as a function of Ir content for different W surface densities.

3.4. Characterization of the Ir-promoted solids *y*Ir/ZSiW*x*

3.4.1. Characterization of the acidity

IR spectra (not shown) were also acquired for *y*Ir/ZSiW*x* solids after exposure to 100 Pa of CO at equilibrium at low temperature. The results show a close similarity of the spectra before and after Ir deposition, indicating little effect of Ir addition on the acidity of the solids. For the 1.2Ir/ZSiW0 solid, a new band at around 2094 cm^{-1}, attributed to the vibration of CO adsorbed on Ir [22–25], was observed. This band was not detected in the spectra of W-rich solids, reflecting low dispersion of the Ir phase in these catalysts.

3.4.2. Characterization of the metallic function

3.4.2.1. Toluene hydrogenation

Structural insensitivity The hydrogenation of toluene is typically considered a structure-insensitive reaction [26,27]. Thus, the turnover frequency (TOF) varies little with the metal particle size, and the activity is a function only of the number of active sites (i.e., number of accessible Ir atoms). This has been verified by Cunha and Cruz [28] in the case of silica-supported system for Ir particle sizes of 1–7 nm. It should be noted, however [28,29] that smaller Ir clusters have been shown to exhibit lower TOF (by one or two orders of magnitude) than those measured for large Ir particles.

Effect of Ir and W content Fig. 8 shows the toluene hydrogenation rates for *y*Ir/ZSiW0, *y*Ir/ZSiW1.5, and *y*Ir/ZSiW3.4 solids ($y = 0.3$, 0.6 and 1.2) as a function of Ir loading. For the ZSiW0 support, the hydrogenation rate can be considered as directly proportional to Ir content. For the *y*Ir/ZSiW1.5 and yIr/ZSiW3.4 solids, a linear increase in the activity with increasing Ir content was also observed. However, toluene hydrogenation activity was detected only above a threshold of Ir loading (ca. 0.25 wt%). Fig. 9 shows the evolution of the rate

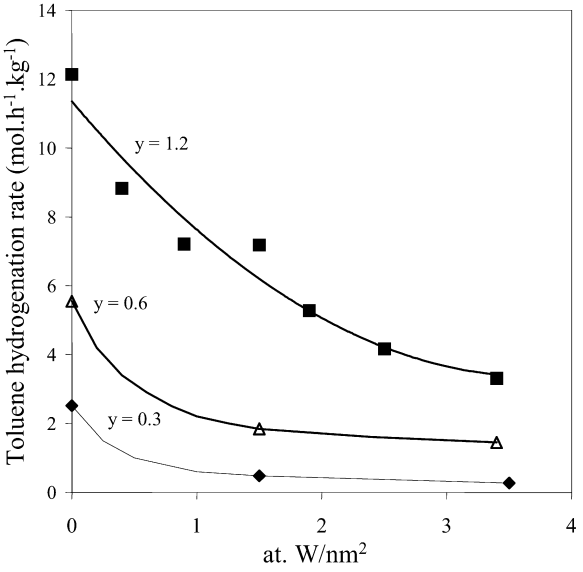

Fig. 9. Evolution of toluene hydrogenation rate as a function of W surface density for different Ir content. The result for the solid 0.6Ir/ZSiW3.4 has been corrected to account for a slightly higher Ir content indicated by atomic absorption measurements.

for toluene hydrogenation as a function of W surface density for varying Ir content. The results clearly show that for a given Ir loading, the rate decreases with increasing W surface density.

3.4.2.2. Characterization of the metallic function by CO adsorption at ambient temperature followed by IR spectroscopy

The metallic function was characterized by CO adsorption at ambient temperature followed by IR spectroscopy. It has been previously shown [7] that for Pd/Al_2O_3 catalysts, the dispersion of the metallic phase can be estimated from the area of the IR bands attributed to CO adsorbed on metallic centers. A similar

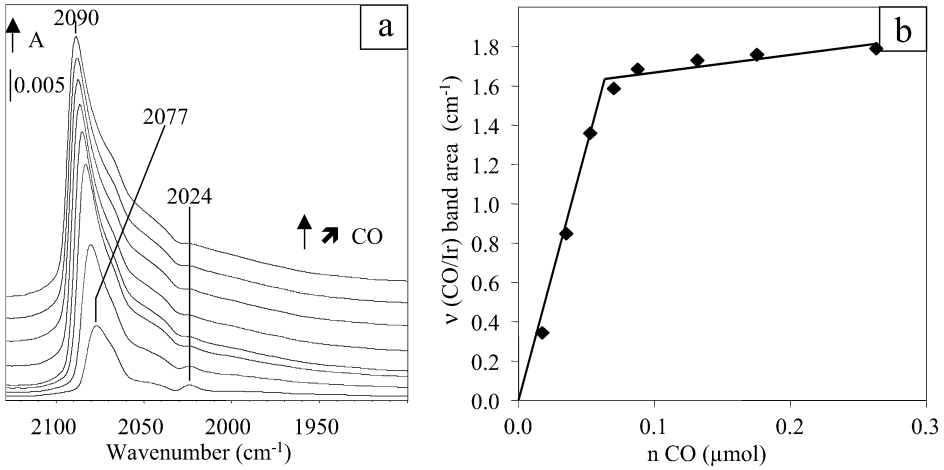

Fig. 10. Infrared spectra for the solid 0.6Ir/ZSiW0 obtained during exposure to increasing doses of CO at ambient temperature (a). Area of the infrared band characteristic of CO interacting with Ir as a function of the amount of CO introduced (b).

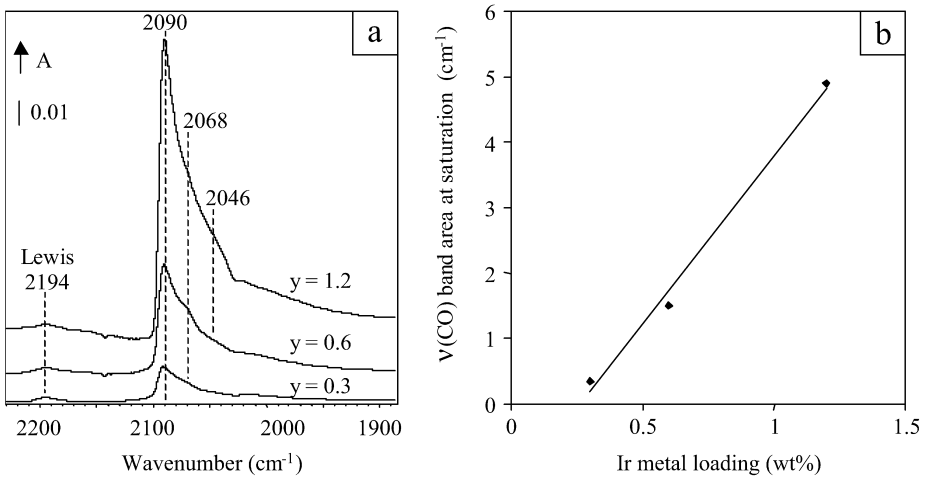

Fig. 11. Infrared spectra for different *y*Ir/ZSiW0 catalysts following exposure to 100 Pa of CO at equilibrium at ambient temperature (a). Evolution of the area of the band as a function of Ir content (b).

approach was used by Duchet and coworkers [4,8] to estimate Pt dispersion in Pt-promoted sulfated or tungstated zirconia catalysts. The position of the band was reportedly a function of the metal particle size [22,30].

Effect of Ir content on the dispersion for yIr/ZSiW0 catalysts Fig. 10a shows for the 0.6Ir/ZSiW0 catalyst, the evolution of IR spectra during incremental addition of CO. The spectral region between 1900 and 2100 cm^{-1} is characteristic of the stretching vibration of CO molecules interacting with Ir metal. The position of the main band shifts from 2077 to 2090 cm^{-1} with the addition of CO. Fig. 10b shows the variation of the area of the band attributed to CO adsorbed on Ir as a function of CO dose. A linear increase (with intercept at the origin) in the area with increasing CO doses up to 0.06 µmol is observed, followed by a much slower increase (also taken as linear) for higher CO doses. The area of the CO band adsorbed on the Ir metal at saturation of the surface was determined from the intersection of the two straight lines. The proposed method [7] assumes that up to saturation of the metallic surface, the added CO molecules adsorb exclusively on the metal, and that the molar absorption coefficients for different carbonyl bands are identical.

The determination of the dispersion of the Ir phase requires knowledge of the stoichiometry of CO adsorption on Ir. McVicker et al. reported that the number of CO molecules adsorbed per Ir atom varies from 1 for atomically dispersed Ir to 2 for Ir particles of 2 nm [22]. A stoichiometry of 0.9–1.5 molecules of CO per Ir atom was reported by Gélin [31]. IR spectra reported by Solymosi et al. [32] and Gélin et al. [23] show the presence of bands of comparable intensity at 2107–2085 and 2037–2000 cm^{-1} attributed to Ir dicarbonyl species. In the present study, analysis of the IR spectra did not indicate the presence of these bands, suggesting limited or no formation of dicarbonyl. Thus a stoichiometry of CO adsorption of 1 was adopted in the present study for all catalysts. On this basis, a dispersion of 13% was calculated for *y*Ir/ZSiW0 catalysts ($y = 0.3$, 0.6, and 1.2).

Fig. 11a shows the IR spectra for the *y*Ir/ZSiW0 catalysts ($y = 0.3$, 0.6, and 1.2) after exposure to 100 Pa of CO at equilibrium at ambient temperature. The band at ca. 2194 cm^{-1} is

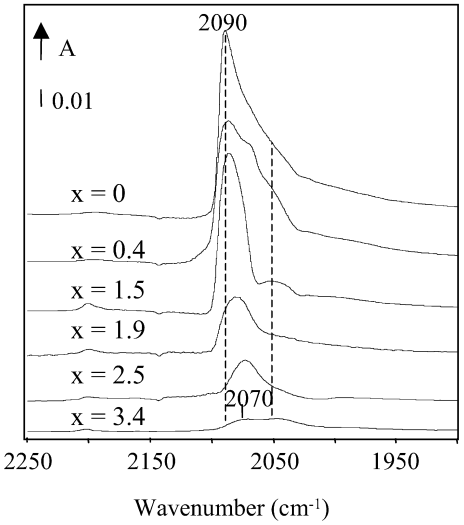

Fig. 12. Infrared spectra for 1.2Ir/ZSiWx catalysts exposed to 100 Pa of CO at equilibrium at ambient temperature.

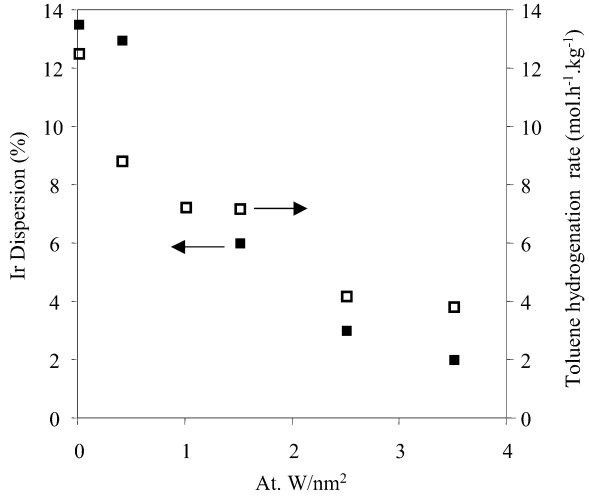

Fig. 13. Ir dispersion (left Y-axis) and toluene hydrogenation rate (right Y-axis) as a function of W surface density for 1.2Ir/ZSiWx solids.

attributed to CO adsorbed on a Lewis acid site. The envelope between 1900 and 2100 cm^{-1}, ascribed to the stretching vibration of CO adsorbed on Ir, consists of a main band at 2090 cm^{-1} and two shoulders at 2068 and 2046 cm^{-1}. Fig. 11b shows that the area of the band attributed to CO adsorbed on Ir at saturation increases linearly with Ir content.

Influence of W surface density on the dispersion of 1.2Ir/ZSiWx catalysts Fig. 12 shows the IR spectra for the 1.2Ir/ZSiWx series after exposure to 100 Pa of CO at equilibrium at ambient temperature. The total spectral area relative to CO adsorption on Ir decreases with increasing the W surface density. This indicates a decrease in the dispersion of the Ir phase. The signal attributed to the vibration of CO adsorbed on Ir consists of several components. The position of the main band decreases from 2090 cm^{-1} for the solid 1.2Ir/ZSiW0 to 2070 cm^{-1} for the 1.2Ir/ZSiW3.4. Dispersion of the Ir phase for the 1.2Ir/ZSiWx catalysts was estimated from the results of CO adsorption at ambient temperature using the method proposed by Binet et al. [7]. Fig. 13 shows the evolution of the Ir dispersion as a function of W surface density. The results indicate a rapid decrease in Ir dispersion with increasing W surface density up to 1.9 at W/nm^2, followed by a slower decrease for higher W surface densities.

4. Discussion

4.1. Characterization of the ZSiWx series

4.1.1. Texture and structure of the support

BET surface area measurements and XRD data illustrate the role of Si in stabilizing the surface area and tetragonal form of the support. The minor presence of monoclinic zirconia in ZSiW0, ZSiW1.5, and ZSiW3.5 suggests less effective stabilisation for these materials. This can be ascribed to the use of two different batches of Si-stabilized zirconia for the preparation of these solids (see Section 2).

4.1.2. Structure of W species

As noted in the Results section, the 950–1050 cm^{-1} region of the IR spectra is characteristic of the ν(W=O) vibration of W surface species. The position of the band was associated with the extent of polymerisation of these species [33]. The spectra of Fig. 3 show bands characteristic of W surface species at 1024 and 1015 cm^{-1} [4,14]; however, in the present study, it is difficult to analyse the evolution of the nature of W species with W surface density due to the overlap with more intense Si bands.

The IR spectra of the ZSiWx solids (Fig. 3) show an increased presence of Si in SiO_2-like environment with increasing W surface density. This has been verified in independent ^{29}Si NMR experiments showing that W addition causes a progressive evolution of the Si environment from isolated toward that of silica-like species. This can be tentatively attributed to partial replacement of Si by W species during impregnation and subsequent aggregation of SiO_2-like domains on the zirconia support.

4.1.3. Acidity

The IR spectrum for the modified zirconia support ZSiW0 shows the band characteristic of the ν(OH) vibration at around 3675 cm^{-1} (Fig. 2). For tungstated zirconia ZSiWx, low-temperature CO adsorption studies indicated that the band at ca. 2172 cm^{-1} is associated with the hydroxyl band at 3565 cm^{-1}. The high wavenumber observed for the CO vibration (2172 cm^{-1}) indicates an interaction with a strong Brønsted acid site.

Comparing Figs. 4a and 4b indicates that W addition causes a decrease in the number of Lewis acid sites (a decrease in the total area attributed to Lewis acid sites) and an increase in their strength (increase in the wavenumber from 2177 cm^{-1} for ZSiW0 to 2189 cm^{-1} for ZSiW3.4). Similarly, the appearance of the bands at 2170 and 2165 cm^{-1} indicates the increased strength of Brønsted acid sites after addition of W. This is illustrated by the results of the decomposition of the IR spectra for ZSiWx solids (Fig. 6) which show that the abundance of

strong (band at ca. 2175 cm^{-1}) and relatively strong (band at 2167 cm^{-1}) Brønsted acid sites increases linearly with W surface density.

4.2. Characterization of the Ir/ZSiWx series

4.2.1. Texture, structure, and acidity

BET surface areas measurements and XRD results indicate that the texture and structure of the solids were not significantly affected on Ir addition. Similarly, as indicated earlier, analysis of the IR spectra for the 1.2Ir/ZSiWx indicates that Ir deposition had little or no impact on the acidity of the solids.

4.2.2. Dispersion of the Ir phase

4.2.2.1. yIr/ZSiW0 catalysts Fig. 8 shows that the rate for toluene hydrogenation of the solids yIr/ZSiW0 is directly proportional to Ir loading, indicating a constant dispersion of the Ir phase. This is in accordance with the dispersion results estimated by IR study of CO adsorption [7]. Note that the latter study also demonstrated that the relative intensities of the bands associated with CO adsorbed on Ir (bands at ca. 2090, 2068, and 2046 cm^{-1}) remained essentially the same for the Ir loadings examined. According to the literature [34–36], high-wavenumber ν(CO) vibrations (2060–2080 cm^{-1}) are attributed to CO adsorbed on large Ir particles, whereas adsorption on small Ir particles is characterized by low-wavenumber vibrations (2020 cm^{-1}). The spectra of Fig. 11a show no significant variation of the location and the intensity of the bands at 2090, 2068, and 2046 cm^{-1} with Ir content. This is consistent with the similarity of Ir dispersion in these solids, indicated by toluene hydrogenation and IR results. Further, the high wavenumber observed for the main peak at 2090 cm^{-1} is coherent with the low dispersion of Ir in these solids.

4.2.2.2. yIr/ZSiW1.5 and yIr/ZSiW3.4 catalysts Fig. 8 shows that the toluene hydrogenation rate increases linearly with Ir loading for the yIr/ZSiW1.5 and yIr/ZSiW3.4 series. However, the intercept does not pass by the origin. A similar result was reported by Vu et al. [4] for the corresponding Pt system and was attributed to an insertion of a finite amount of Pt in the zirconia matrix. This hypothesis does not appear likely in the present study, however, because no such behaviour was observed for the W-free system. This suggests that the presence of a threshold for the development of hydrogenation activity is associated with an interaction of a fraction of Ir with W leading to a decrease in the intrinsic hydrogenation activity of the Ir phase.

4.2.2.3. Ir/ZSiWx catalysts Fig. 9 shows that the toluene hydrogenation rate decreased with the surface density of W. This can be attributed to a decrease in the dispersion of the Ir or of the intrinsic hydrogenation activity of Ir. The first hypothesis is supported by the parallel evolution of the activity and dispersion of Ir with W surface density (Fig. 13).

5. Conclusion

The acidity of Si-stabilized tungstated zirconia solids ZSiWx was monitored by low-temperature CO adsorption followed by IR spectroscopy. The results indicated the development of strong and relatively strong Brønsted acidity with increasing W surface density above a threshold of 1 atom W/nm^2. The study of the Ir-doped solids showed that the texture, structure, and acidity of the ZSiWx solids were not affected by Ir deposition.

Characterization of the metallic function was performed by hydrogenation of toluene and by CO adsorption at ambient temperature, followed by IR spectroscopy. Both methods indicated a low and constant Ir dispersion for the yIr/ZSiW0 ($y = 0.3$, 0.6, 1.2) series. For a given Ir loading (1.2Ir/ZSiWx), a progressive decrease in the dispersion of Ir metal with increasing W surface density was observed.

References

[1] G.B. McVicker, M. Daage, M.S. Touvelle, C.W. Hudson, D.P. Klein, W.C. Baird, B.R. Cook, J.G. Chen, S. Hantzer, D.E.W. Vaughan, E.S. Ellis, O.C. Feeley, J. Catal. 210 (2002) 137.
[2] H. Schultz, J. Weitkamp, H. Eberth, in: J.W. Hightower (Ed.), Proc. 5th Int. Congr. Catal., vol. 2, North-Holland, Amsterdam, 1972, p. 1229.
[3] G. Onyestyak, G. Pal-Borbély, H.K. Beyer, Appl. Catal. A 229 (2002) 65.
[4] T.N. Vu, J. van Gestel, J.P. Gilson, C. Collet, J.P. Dath, J.C. Duchet, J. Catal. 231 (2005) 453.
[5] H. Toraya, Y. Yoshimura, S. Somiya, J. Am. Ceram. Soc. 67 (1984) 119.
[6] H.P. Klug, L.E. Alexander, X-Ray Diffraction Procedures, Wiley, New York, 1974.
[7] C. Binet, A. Jadi, J.C. Lavalley, J. Chim. Phys. 86 (1989) 451.
[8] J. van Gestel, T.N. Vu, D. Guillaume, J.P. Gilson, J.C. Duchet, J. Catal. 212 (2002) 173.
[9] O. Cairon, T. Chevreau, J.C. Lavalley, J. Chem. Soc. Faraday Trans. 94 (1998) 3039.
[10] O. Cairon, K. Thomas, A. Chambellan, T. Chevreau, Appl. Catal. A 238 (2003) 167.
[11] C. Morterra, G. Cerrato, L. Ferroni, Mater. Chem. Phys. 37 (1994) 243.
[12] C. Morterra, G. Cerrato, S. Di Ciero, Appl. Surf. Sci. 126 (1998) 107.
[13] A. Burneau, J.P. Gallas, in: A.P. Legrand (Ed.), The Surface Properties of Silica, Wiley, New York, 1998.
[14] M. Scheithauer, R.K. Grasselli, H. Knözinger, Langmuir 14 (1998) 3019.
[15] J.C. Lavalley, S. Jolly-Feaugas, A. Janin, J. Saussey, Mikrochim. Acta 14 (1997) 51.
[16] M.I. Zaki, H. Knözinger, Spectrochim. Acta A 43 (12) (1987) 1455.
[17] L.M. Kustov, V.B. Kazansky, S. Beran, L. Kubelkova, P. Juri, J. Phys. Chem. 91 (1987) 5247.
[18] L. Kubelkova, S. Beran, J.A. Lercher, Zeolites 9 (1989) 539.
[19] G. Ferraris, S. De Rossi, D. Gazzoli, I. Pettiti, M. Valigi, G. Magnacca, C. Morterra, Appl. Catal. A 240 (2003) 119.
[20] M.I. Zaki, H. Knözinger, Mater. Chem. Phys. 17 (1987) 201.
[21] O. Cairon, K. Thomas, T. Chevreau, Microporous Mesoporous Mater. 46 (2001) 327.
[22] G.B. McVicker, R.T.K. Baker, R.L. Garten, E.L. Kugler, J. Catal. 65 (1980) 207.
[23] P. Gélin, A. Auroux, Y. Ben Taarit, P.C. Gravelle, Appl. Catal. 46 (1989) 227.
[24] C.R. Guerra, J.H. Schulman, Surf. Sci. 7 (1967) 229.
[25] A. Bourane, M. Nawdali, D. Bianchi, J. Phys. Chem. B 106 (2002) 2665.
[26] M. Boudart, G. Djéga-Mariadassou, Kinetics of Heterogeneous Catalytic Reactions, Princeton Univ. Press, Princeton, NJ, 1984.
[27] M. Che, C.O. Bennett, Adv. Catal. 36 (1989) 55.
[28] D.S. Cunha, G.M. Cruz, Appl. Catal. A 236 (2002) 55.
[29] O. Alexeev, B.C. Gates, J. Catal. 176 (1998) 310.

[30] L.C. de Ménorval, A. Chaqroune, B. Coq, F. Figueras, J. Chem. Soc. Faraday Trans. 93 (1997) 3715.
[31] P. Gélin, Ph.D. thesis, Université Claude Bernard-Lyon (1981).
[32] F. Solymosi, E. Novak, A. Molhar, J. Phys. Chem. 94 (1990) 7250.
[33] S. Eibl, B.C. Gates, H. Knözinger, Langmuir 17 (2001) 107.
[34] F.J.C.M. Toolenaar, A.G.T.M. Bastein, V. Ponec, J. Catal. 82 (1983) 35.
[35] R.F. Howe, J. Catal. 50 (1977) 196.
[36] F. Solymosi, J. Rasko, J. Catal. 62 (1980) 253.